desired earnestly. Where the viscous correction means viscous drag and circulation reduction around blade section by the effect of the boundary layer.

It goes without saying that the experimental data are very important for the evaluation of the surface panel method. Dr. Jessup's experimental data presented in his dissertation contributes to our plan. One of the calculation propellers is the same as the one to be used in the comparative experiments for viscous effects, also organized by the 20th ITTC Propulsor Committee.

20th ITTC Propulsor Committee
Comparative Calculation of Propellers by Surface Panel Method

1. Input Data sent here

1.1. Geometry of the propellers

DTRC Prop.4119

Photo	Fig.1.1.1
Blade	Table 1.1.1
Hub	Fig.1.1.2

DTRC Prop.4842

Photo	Fig.1.1.1
Blade	Table 1.1.2
Hub	Fig.1.1.2

1.2. Calculation conditions

in uniform flow

DTRC Prop.4119	Advance Coeficient	J=0.833 , n=10rps
		J=1.100 , n=10rps
DTRC Prop.4842	Advance Coeficient	J=0.905 , n=10rps

* detail and priority of the standard calculation condition are shown in Table 1.2.1

1.3. Experimental data for the reference (Jessup's experiment)

DTRC Prop.4119

KT, KQ	Fig.1.3.1
	Table 1.3.1
CP	Fig.1.3.3
blade wake	Fig.1.3.4
section drag	Fig.1.3.5

DTRC Prop.4842

KT, KQ	Fig.1.3.2
	Table 1.3.1

* If you want Dr.Jessup's dissertation "An Experimental Investigation of Viscous Aspects of Propeller Blade Flow", please ask me for it. I can send you the copy.

2. Output Data required to be sent

2.1. Format of the expression for the calculation results

number, distribution (chordwise and radial) and form of panels

$KT = T / \rho\ n^2\ D^4$

$KQ = Q / \rho\ n^2\ D^5$

$CP = 1 - (VV/VR)^2$ at 0.3, 0.7, 0.9 radius

$VR^2 = V^2 + (2\pi nr)^2$

V = advance speed

VV = flow velocity on the blade

blade wake pitch

viscous correction factors (viscous blade section drag and circulation reduction around blade section)

* Calculation results should be presented in the form of tables and figures
* Please explain any conditions if they are different from the standard calculation condition shown in this document. (for example the hub form)

2.2. Method of calculation (Copy of the paper presenting the method)

Theory

Numerical method

2.3. Comments on the calculation results

paneling

Do you have some standard for the number of panels ?

Do you have some standard for the accuracy of KT or CP ?

effect of hub

deformation of blade wake

viscous effect

How do you make the value of the viscous correction factor?

Table 1.1.1 (a) Blade geometry of DTRC4119

xyzprop blade geometry ofDTRC 4119

NUMBER OF BLADES = 3

PROPELLER DIAMETER = 12.0000 INCHES

INPUT SCALED BY LAMDA = 1.0000

	R/R0	R (INCHES)	CHORD (INCHES)	CHORD/D	TAN PHI	PITCH/D	PITCHAN (RADIANS)
0	0.20000	1.2000	3.8400	0.32000	1.75866	1.10500	1.05377
0	0.25000	1.5000	4.1040	0.34200	1.40527	1.10370	0.95232
0	0.30000	1.8000	4.3620	0.36350	1.16947	1.10220	0.86336
0	0.40000	2.4000	4.8576	0.40480	0.87400	1.09830	0.71826
0	0.50000	3.0000	5.2704	0.43920	0.69595	1.09320	0.60800
0	0.60000	3.6000	5.5320	0.46100	0.57715	1.08790	0.52345
0	0.70000	4.2000	5.5464	0.46220	0.49288	1.08390	0.45794
0	0.80000	4.8000	5.2164	0.43470	0.43016	1.08110	0.40623
0	0.90000	5.4000	4.3356	0.36130	0.38144	1.07850	0.36441
0	0.95000	5.7000	3.3300	0.27750	0.36086	1.07700	0.34632
0	1.00000	6.0000	0.0000	0.00000	0.34218	1.07500	0.32969
0	0.92500	5.5500	3.9145	0.32621	0.37089	1.07779	0.35516
0	0.97500	5.8500	2.4538	0.20449	0.35131	1.07609	0.33784
0	0.99000	5.9400	1.5931	0.13276	0.34579	1.07546	0.33292
0	0.99500	5.9700	1.1375	0.09479	0.34398	1.07523	0.33130

	R/R0	TOTAL RAKE/D	SKEWAN (RADIANS)	T/CHORD	FM/CHORD	TE OFFSET (INCHES)
0	0.20000	0.00000	0.00000	0.20550	0.01429	0.00000
0	0.25000	0.00000	0.00000	0.17870	0.01985	0.00000
0	0.30000	0.00000	0.00000	0.15530	0.02318	0.00000
0	0.40000	0.00000	0.00000	0.11800	0.02303	0.00000
0	0.50000	0.00000	0.00000	0.09016	0.02182	0.00000
0	0.60000	0.00000	0.00000	0.06960	0.02072	0.00000
0	0.70000	0.00000	0.00000	0.05418	0.02003	0.00000
0	0.80000	0.00000	0.00000	0.04206	0.01967	0.00000
0	0.90000	0.00000	0.00000	0.03321	0.01817	0.00000
0	0.95000	0.00000	0.00000	0.03228	0.01631	0.00000
0	1.00000	0.00000	0.00000	0.03160	0.01175	0.00000
0	0.92500	0.00000	0.00000	0.03252	0.01744	0.00000
0	0.97500	0.00000	0.00000	0.03211	0.01450	0.00000
0	0.99000	0.00000	0.00000	0.03187	0.01298	0.00000
0	0.99500	0.00000	0.00000	0.03175	0.01239	0.00000

R/R0 = FRACTION OF PROPELLER RADIUS,R0
R = LOCAL RADIUS
CHORD = TOTAL WIDTH OF BLADE SECTION
D = PROPELLER DIAMETER
TAN PHI = TANGENT OF PITCH ANGLE
LAMDA = ARCTAN((TOT RAKE)/(R'SKEWANGLE))
PITCH = BLADE-SECTION PITCH
PITCHAN = PITCH ANGLE
TOT RAKE = AXIAL DISTANCE OF BLADE-SECTION MID-CHORD POINT FROM PLANE PERPE
NDICULAR TO SHAFT AXIS CONTAINING PROPELLER CENTER AXIS(X=0 PLANE)
SKEWAN = SKEWANGLE = CIRCUMFERENTIAL DISPLACEMENT OF BLADE-SECTION MID-CHORD
POINT FROM PLANE THRU SHAFT AXIS CONTAINING PROPELLER CENTER AXIS (Y=0 PLANE)
T = MAX THICKNESS AT RADIUS R
FM = CAMBER AT RADIUS R

Table 1.1.1 (b) Blade geometry of DTRC4119

SECTION OFFSETS
(IN INCHES)

xyz prop blade geometry of DTRC 4119

ORDINATES (NO TRAILING-EDGE MODIFICATIONS) AT NONDIMENSIONAL RADIUS R/R0

FRACTION OF CHORD		0.2000	0.2500	0.3000	0.4000	0.5000	0.6000	0.7000	0.8000
0.000000	U	0.0000	0.0000	0.0000	0.0000	0.0000	0.0000	0.0000	0.0000
	L	0.0000	0.0000	0.0000	0.0000	0.0000	0.0000	0.0000	0.0000
0.010000	U	0.0780	0.0748	0.0710	0.0621	0.0532	0.0447	0.0365	0.0283
	L	-0.0697	-0.0625	-0.0557	-0.0452	-0.0358	-0.0274	-0.0197	-0.0128
0.025000	U	0.1244	0.1204	0.1153	0.1018	0.0879	0.0746	0.0617	0.0484
	L	-0.1070	-0.0946	-0.0833	-0.0663	-0.0514	-0.0383	-0.0264	-0.0159
0.050000	U	0.1779	0.1736	0.1674	0.1488	0.1294	0.1106	0.0922	0.0732
	L	-0.1482	-0.1294	-0.1125	-0.0881	-0.0670	-0.0485	-0.0320	-0.0175
0.100000	U	0.2540	0.2497	0.2422	0.2168	0.1897	0.1633	0.1371	0.1098
	L	-0.2048	-0.1767	-0.1516	-0.1165	-0.0866	-0.0606	-0.0376	-0.0178
0.200000	U	0.3540	0.3503	0.3417	0.3075	0.2705	0.2342	0.1979	0.1595
	L	-0.2773	-0.2364	-0.2003	-0.1510	-0.1097	-0.0739	-0.0425	-0.0160
0.300000	U	0.4134	0.4105	0.4015	0.3624	0.3197	0.2776	0.2353	0.1904
	L	-0.3186	-0.2698	-0.2269	-0.1692	-0.1211	-0.0796	-0.0434	-0.0132
0.400000	U	0.4435	0.4415	0.4327	0.3914	0.3459	0.3009	0.2556	0.2073
	L	-0.3380	-0.2848	-0.2382	-0.1763	-0.1247	-0.0805	-0.0420	-0.0100
0.500000	U	0.4464	0.4454	0.4372	0.3963	0.3508	0.3057	0.2602	0.2115
	L	-0.3367	-0.2824	-0.2350	-0.1725	-0.1208	-0.0764	-0.0380	-0.0063
0.600000	U	0.4209	0.4210	0.4142	0.3762	0.3336	0.2913	0.2485	0.2025
	L	-0.3135	-0.2615	-0.2163	-0.1572	-0.1086	-0.0670	-0.0311	-0.0017
0.700000	U	0.3672	0.3684	0.3632	0.3308	0.2940	0.2573	0.2200	0.1798
	L	-0.2696	-0.2235	-0.1834	-0.1318	-0.0895	-0.0534	-0.0225	0.0027
0.800000	U	0.2840	0.2853	0.2817	0.2569	0.2286	0.2003	0.1715	0.1403
	L	-0.2069	-0.1708	-0.1396	-0.0997	-0.0670	-0.0392	-0.0154	0.0039
0.900000	U	0.1678	0.1669	0.1634	0.1477	0.1304	0.1134	0.0962	0.0780
	L	-0.1284	-0.1084	-0.0909	-0.0675	-0.0480	-0.0312	-0.0166	-0.0044
0.950000	U	0.0996	0.0978	0.0947	0.0847	0.0740	0.0636	0.0534	0.0427
	L	-0.0808	-0.0699	-0.0601	-0.0464	-0.0346	-0.0244	-0.0153	-0.0075
0.975000	U	0.0635	0.0615	0.0590	0.0520	0.0450	0.0382	0.0316	0.0248
	L	-0.0545	-0.0482	-0.0424	-0.0337	-0.0261	-0.0194	-0.0134	-0.0080
0.990000	U	0.0412	0.0392	0.0370	0.0321	0.0273	0.0228	0.0184	0.0141
	L	-0.0378	-0.0342	-0.0308	-0.0253	-0.0203	-0.0158	-0.0117	-0.0079
1.000000	U	0.0263	0.0244	0.0226	0.0191	0.0158	0.0128	0.0100	0.0073
	L	-0.0263	-0.0244	-0.0226	-0.0191	-0.0158	-0.0128	-0.0100	-0.0073

U = OFFSET OF UPPER SURFACE (SUCTION SIDE, SUCTION FACE, BACK) OF BLADE SECTION MEASURED FROM REFERENCE LINE (NOSE-TAIL LINE)

L = OFFSET OF LOWER SURFACE (PRESSURE SIDE, PRESSURE FACE, FACE) OF BLADE SECTION MEASURED FROM REFERENCE LINE (NOSE-TAIL LINE)

Table 1.1.1 (c) Blade geometry of DTRC4119

xyzprop blade geometry ofDTRC 4119

ORDINATES (NO TRAILING-EDGE MODIFICATIONS) AT NONDIMENSIONAL RADIUS R/RO

FRACTION OF CHORD		0.9000	0.9500	1.0000	0.9250	0.9750	0.9900	0.9950
0.000000	U	0.0000	0.0000	0.0000	0.0000	0.0000	0.0000	0.0000
	L	0.0000	0.0000	0.0000	0.0000	0.0000	0.0000	0.0000
0.010000	U	0.0194	0.0142	0.0000	0.0171	0.0101	0.0063	0.0044
	L	-0.0075	-0.0059	0.0000	-0.0067	-0.0047	-0.0032	-0.0023
0.025000	U	0.0336	0.0244	0.0000	0.0295	0.0172	0.0107	0.0075
	L	-0.0086	-0.0071	0.0000	-0.0078	-0.0059	-0.0042	-0.0031
0.050000	U	0.0511	0.0369	0.0000	0.0448	0.0259	0.0161	0.0113
	L	-0.0084	-0.0075	0.0000	-0.0078	-0.0066	-0.0049	-0.0036
0.100000	U	0.0772	0.0556	0.0000	0.0676	0.0389	0.0240	0.0168
	L	-0.0065	-0.0069	0.0000	-0.0064	-0.0070	-0.0055	-0.0042
0.200000	U	0.1127	0.0810	0.0000	0.0987	0.0564	0.0348	0.0243
	L	-0.0025	-0.0050	0.0000	-0.0032	-0.0066	-0.0058	-0.0046
0.300000	U	0.1348	0.0968	0.0000	0.1180	0.0673	0.0414	0.0289
	L	0.0012	-0.0030	0.0000	-0.0001	-0.0058	-0.0057	-0.0046
0.400000	U	0.1470	0.1055	0.0000	0.1287	0.0732	0.0450	0.0314
	L	0.0044	-0.0010	0.0000	0.0026	-0.0048	-0.0053	-0.0043
0.500000	U	0.1502	0.1077	0.0000	0.1314	0.0747	0.0459	0.0320
	L	0.0073	0.0010	0.0000	0.0051	-0.0035	-0.0045	-0.0038
0.600000	U	0.1441	0.1032	0.0000	0.1260	0.0715	0.0439	0.0306
	L	0.0101	0.0031	0.0000	0.0076	-0.0018	-0.0034	-0.0030
0.700000	U	0.1281	0.0917	0.0000	0.1121	0.0634	0.0389	0.0271
	L	0.0120	0.0049	0.0000	0.0094	-0.0001	-0.0021	-0.0020
0.800000	U	0.1001	0.0716	0.0000	0.0876	0.0495	0.0303	0.0211
	L	0.0106	0.0047	0.0000	0.0084	0.0005	-0.0013	-0.0013
0.900000	U	0.0553	0.0397	0.0000	0.0484	0.0275	0.0169	0.0118
	L	0.0012	-0.0007	0.0000	0.0006	-0.0020	-0.0021	-0.0017
0.950000	U	0.0300	0.0216	0.0000	0.0262	0.0151	0.0093	0.0065
	L	-0.0030	-0.0030	0.0000	-0.0029	-0.0029	-0.0023	-0.0017
0.975000	U	0.0172	0.0125	0.0000	0.0151	0.0088	0.0055	0.0039
	L	-0.0043	-0.0036	0.0000	-0.0039	-0.0030	-0.0021	-0.0015
0.990000	U	0.0096	0.0070	0.0000	0.0084	0.0050	0.0032	0.0022
	L	-0.0048	-0.0037	0.0000	-0.0043	-0.0029	-0.0019	-0.0014
1.000000	U	0.0048	0.0036	0.0000	0.0042	0.0026	0.0017	0.0012
	L	-0.0048	-0.0036	0.0000	-0.0042	-0.0026	-0.0017	-0.0012

U = OFFSET OF UPPER SURFACE (SUCTION SIDE, SUCTION FACE, BACK) OF BLADE SECTION MEASURED FROM REFERENCE LINE (NOSE-TAIL LINE)

L = OFFSET OF LOWER SURFACE (PRESSURE SIDE, PRESSURE FACE, FACE) OF BLADE SECTION MEASURED FROM REFERENCE LINE (NOSE-TAIL LINE)

Table 1.1.2 (a) Blade geometry of DTRC4842

xyz prop blade geometry of DTRC 4842

NUMBER OF BLADES = 5

PROPELLER DIAMETER = 14.6280 INCHES

INPUT SCALED BY LAMDA = 1.0000

	R/R0	R (INCHES)	CHORD (INCHES)	CHORD/D	TAN PHI	PITCH/D	PITCHAN (RADIANS)
0	0.32300	2.3624	2.9475	0.20150	0.91857	0.93210	0.74298
0	0.35000	2.5599	3.1904	0.21810	0.98130	1.07900	0.77596
0	0.40000	2.9256	3.6482	0.24940	0.98366	1.23610	0.77716
0	0.50000	3.6570	4.5537	0.31130	0.90362	1.41940	0.73481
0	0.60000	4.3884	5.3597	0.36640	0.79005	1.48920	0.66864
0	0.70000	5.1198	5.8965	0.40310	0.67664	1.48800	0.59487
0	0.80000	5.8512	5.9829	0.40900	0.52879	1.32900	0.48642
0	0.90000	6.5826	5.3407	0.36510	0.38052	1.07590	0.36360
0	0.95000	6.9483	4.5435	0.31060	0.30196	0.90120	0.29325
0	1.00000	7.3140	1.0240	0.07000	0.22221	0.69810	0.21866
0	0.92500	6.7655	5.0102	0.34251	0.34164	0.99280	0.32921
0	0.97500	7.1312	3.7849	0.25875	0.26199	0.80250	0.25624
0	0.99000	7.2409	2.9400	0.20098	0.23808	0.74046	0.23372
0	0.99500	7.2774	2.4436	0.16705	0.23013	0.71937	0.22619

	R/R0	TOTAL RAKE/D	SKEWAN (RADIANS)	T/CHORD	FM/CHORD	TE OFFSET (INCHES)
0	0.32300	0.00005	0.00663	0.21790	0.01000	0.00000
0	0.35000	0.00020	-0.05358	0.18710	0.01580	0.00000
0	0.40000	0.00053	-0.11903	0.14150	0.02530	0.00000
0	0.50000	-0.00144	-0.15743	0.08540	0.03650	0.00000
0	0.60000	-0.00122	-0.13212	0.05810	0.03900	0.00000
0	0.70000	-0.00021	-0.05655	0.04440	0.03710	0.00000
0	0.80000	0.00040	0.07575	0.03790	0.03190	0.00000
0	0.90000	0.00123	0.23998	0.03560	0.02640	0.00000
0	0.95000	0.00272	0.33598	0.03630	0.02470	0.00000
0	1.00000	0.00684	0.44366	0.08800	0.02430	0.00000
0	0.92500	0.00177	0.28661	0.03325	0.02542	0.00000
0	0.97500	0.00433	0.38827	0.05210	0.02431	0.00000
0	0.99000	0.00571	0.42112	0.07076	0.02425	0.00000
0	0.99500	0.00625	0.43233	0.07886	0.02427	0.00000

R/R0 = FRACTION OF PROPELLER RADIUS,R0
R = LOCAL RADIUS
CHORD = TOTAL WIDTH OF BLADE SECTION
D = PROPELLER DIAMETER
TAN PHI = TANGENT OF PITCH ANGLE
LAMDA = ARCTAN((TOT RAKE)/(R'SKEWANGLE))
PITCH = BLADE-SECTION PITCH
PITCHAN = PITCH ANGLE
TOT RAKE = AXIAL DISTANCE OF BLADE-SECTION MID-CHORD POINT FROM PLANE PERPENDICULAR TO SHAFT AXIS CONTAINING PROPELLER CENTER AXIS(X=0 PLANE)
SKEWAN = SKEWANGLE = CIRCUMFERENTIAL DISPLACEMENT OF BLADE-SECTION MID-CHORD POINT FROM PLANE THRU SHAFT AXIS CONTAINING PROPELLER CENTER AXIS (Y=0 PLANE)
T = MAX THICKNESS AT RADIUS R

Table 1.1.2 (b) Blade geometry of DTRC4842

SECTION OFFSETS
(IN INCHES)

xyz prop blade geometry of DTRC 4842

ORDINATES (NO TRAILING-EDGE MODIFICATIONS) AT NONDIMENSIONAL RADIUS R/R0

FRACTION OF CHORD		0.3230	0.3500	0.4000	0.5000	0.6000	0.7000	0.8000
0.000000	U	0.0000	0.0000	0.0000	0.0000	0.0000	0.0000	0.0000
	L	0.0000	0.0000	0.0000	0.0000	0.0000	0.0000	0.0000
0.010000	U	0.0622	0.0595	0.0550	0.0485	0.0444	0.0404	0.0351
	L	-0.0579	-0.0522	-0.0416	-0.0243	-0.0139	-0.0085	-0.0073
0.025000	U	0.0987	0.0952	0.0898	0.0824	0.0776	0.0719	0.0624
	L	-0.0896	-0.0798	-0.0616	-0.0316	-0.0137	-0.0049	-0.0040
0.050000	U	0.1404	0.1366	0.1309	0.1240	0.1192	0.1115	0.0969
	L	-0.1250	-0.1101	-0.0824	-0.0367	-0.0095	0.0033	0.0033
0.100000	U	0.1997	0.1958	0.1908	0.1864	0.1828	0.1727	0.1502
	L	-0.1737	-0.1513	-0.1093	-0.0397	0.0018	0.0205	0.0183
0.200000	U	0.2774	0.2738	0.2707	0.2712	0.2699	0.2569	0.2234
	L	-0.2364	-0.2037	-0.1423	-0.0400	0.0208	0.0474	0.0420
0.300000	U	0.3233	0.3204	0.3191	0.3238	0.3248	0.3102	0.2699
	L	-0.2724	-0.2333	-0.1598	-0.0369	0.0360	0.0674	0.0595
0.400000	U	0.3464	0.3441	0.3445	0.3526	0.3555	0.3403	0.2961
	L	-0.2897	-0.2471	-0.1667	-0.0325	0.0471	0.0810	0.0715
0.500000	U	0.3482	0.3466	0.3485	0.3592	0.3635	0.3487	0.3034
	L	-0.2892	-0.2458	-0.1639	-0.0268	0.0545	0.0889	0.0783
0.600000	U	0.3276	0.3269	0.3302	0.3430	0.3487	0.3351	0.2916
	L	-0.2701	-0.2286	-0.1502	-0.0189	0.0589	0.0915	0.0806
0.700000	U	0.2850	0.2851	0.2893	0.3028	0.3091	0.2976	0.2590
	L	-0.2333	-0.1966	-0.1273	-0.0110	0.0578	0.0864	0.0760
0.800000	U	0.2197	0.2197	0.2229	0.2333	0.2381	0.2293	0.1995
	L	-0.1798	-0.1516	-0.0982	-0.0086	0.0445	0.0665	0.0585
0.900000	U	0.1312	0.1303	0.1302	0.1330	0.1340	0.1282	0.1115
	L	-0.1099	-0.0938	-0.0635	-0.0129	0.0171	0.0299	0.0264
0.950000	U	0.0787	0.0772	0.0755	0.0741	0.0729	0.0690	0.0600
	L	-0.0682	-0.0592	-0.0425	-0.0148	0.0017	0.0091	0.0081
0.975000	U	0.0505	0.0489	0.0463	0.0430	0.0408	0.0379	0.0329
	L	-0.0456	-0.0404	-0.0309	-0.0152	-0.0058	-0.0013	-0.0010
0.990000	U	0.0329	0.0312	0.0283	0.0240	0.0213	0.0191	0.0165
	L	-0.0313	-0.0285	-0.0233	-0.0149	-0.0099	-0.0071	-0.0061
1.000000	U	0.0214	0.0199	0.0172	0.0129	0.0104	0.0087	0.0076
	L	-0.0214	-0.0199	-0.0172	-0.0129	-0.0104	-0.0087	-0.0076

U = OFFSET OF UPPER SURFACE (SUCTION SIDE, SUCTION FACE, BACK) OF BLADE SECTION MEASURED FROM REFERENCE LINE (NOSE-TAIL LINE)
L = OFFSET OF LOWER SURFACE (PRESSURE SIDE, PRESSURE FACE, FACE) OF BLADE SECTION MEASURED FROM REFERENCE LINE (NOSE-TAIL LINE)

Table 1.1.2 (c) Blade geometry of DTRC4842

xyz prop blade geometry of DTRC 4842

ORDINATES (NO TRAILING-EDGE MODIFICATIONS) AT NONDIMENSIONAL RADIUS R/RO

FRACTION OF CHORD		0.9000	0.9500	1.0000	0.9250	0.9750	0.9900	0.9950
0.000000	U	0.0000	0.0000	0.0000	0.0000	0.0000	0.0000	0.0000
	L	0.0000	0.0000	0.0000	0.0000	0.0000	0.0000	0.0000
0.010000	U	0.0281	0.0236	0.0102	0.0249	0.0252	0.0247	0.0224
	L	-0.0075	-0.0073	-0.0066	-0.0063	-0.0117	-0.0143	-0.0137
0.025000	U	0.0494	0.0413	0.0170	0.0439	0.0430	0.0414	0.0373
	L	-0.0063	-0.0070	-0.0094	-0.0049	-0.0148	-0.0196	-0.0192
0.050000	U	0.0763	0.0635	0.0251	0.0678	0.0649	0.0617	0.0554
	L	-0.0023	-0.0046	-0.0121	-0.0010	-0.0166	-0.0243	-0.0242
0.100000	U	0.1175	0.0975	0.0372	0.1046	0.0980	0.0920	0.0822
	L	0.0070	0.0016	-0.0152	0.0078	-0.0167	-0.0290	-0.0298
0.200000	U	0.1741	0.1440	0.0533	0.1552	0.1429	0.1328	0.1183
	L	0.0220	0.0121	-0.0187	0.0219	-0.0149	-0.0336	-0.0358
0.300000	U	0.2099	0.1733	0.0633	0.1871	0.1709	0.1580	0.1406
	L	0.0335	0.0204	-0.0203	0.0326	-0.0121	-0.0349	-0.0382
0.400000	U	0.2299	0.1897	0.0686	0.2051	0.1863	0.1717	0.1525
	L	0.0416	0.0264	-0.0207	0.0401	-0.0091	-0.0343	-0.0383
0.500000	U	0.2353	0.1941	0.0696	0.2100	0.1899	0.1745	0.1549
	L	0.0467	0.0304	-0.0198	0.0447	-0.0058	-0.0319	-0.0363
0.600000	U	0.2259	0.1862	0.0662	0.2017	0.1815	0.1663	0.1475
	L	0.0490	0.0327	-0.0177	0.0466	-0.0021	-0.0273	-0.0318
0.700000	U	0.2005	0.1650	0.0582	0.1790	0.1603	0.1465	0.1298
	L	0.0470	0.0320	-0.0145	0.0446	0.0012	-0.0214	-0.0257
0.800000	U	0.1544	0.1272	0.0448	0.1379	0.1235	0.1129	0.1000
	L	0.0362	0.0246	-0.0112	0.0343	0.0009	-0.0165	-0.0198
0.900000	U	0.0866	0.0715	0.0259	0.0773	0.0703	0.0648	0.0576
	L	0.0153	0.0096	-0.0079	0.0147	-0.0038	-0.0133	-0.0147
0.950000	U	0.0469	0.0389	0.0147	0.0418	0.0390	0.0365	0.0326
	L	0.0034	0.0012	-0.0059	0.0037	-0.0061	-0.0111	-0.0114
0.975000	U	0.0260	0.0217	0.0088	0.0231	0.0225	0.0215	0.0194
	L	-0.0024	-0.0029	-0.0047	-0.0018	-0.0070	-0.0096	-0.0094
0.990000	U	0.0134	0.0113	0.0052	0.0118	0.0124	0.0124	0.0113
	L	-0.0057	-0.0052	-0.0038	-0.0049	-0.0074	-0.0085	-0.0080
1.000000	U	0.0063	0.0055	0.0030	0.0055	0.0066	0.0069	0.0064
	L	-0.0063	-0.0055	-0.0030	-0.0055	-0.0066	-0.0069	-0.0064

U = OFFSET OF UPPER SURFACE (SUCTION SIDE, SUCTION FACE, BACK) OF BLADE SECTION MEASURED FROM REFERENCE LINE (NOSE-TAIL LINE)
L = OFFSET OF LOWER SURFACE (PRESSURE SIDE, PRESSURE FACE, FACE) OF BLADE SECTION MEASURED FROM REFERENCE LINE (NOSE-TAIL LINE)

Table 1.2.1. Details and priorities of the standard calculation condition

			order of priority
Prop.4119 J=0.833			
recomended paneling	without hub	linear wake	1
reference paneling	without hub	linear wake	4
recomended paneling	with hub	linear wake	5
recomended paneling	without hub	devised wake	6
recomended paneling	with hub	devised wake	2
Prop.4119 J=1.100			
recomended paneling	without hub	linear wake	7
recomended paneling	without hub	devised wake	8
Prop.4842 J=0.905			
recommended paneling	with hub	devised wake	3

recommended paneling	you recommend or you use
reference paneling	fine or course or lower order or higher order paneling which shows the validation of the paneling you recommend
linear wake	blade vortex wake remains its location at the point it has emanated in spite of induced velocity
devised wake	modeled wake calculated wake

Table 1.3.1 Open water test results for DTRC4119 and DTRC4842

Propeller 4119

OPEN WATER RESULTS			
J	K_T	$10K_Q$	η_o
0.5	0.285	0.477	0.489
0.7	0.200	0.360	0.632
0.833	0.146	0.280	0.692
0.9	0.120	0.239	0.725
1.1	0.034	0.106	0.575
DESIGN LOADS			
0.833	0.154	0.290	0.706

Propeller 4842

OPEN WATER RESULTS			
J	K_T	$10K_Q$	η_o
0.5	0.496	0.995	0.397
0.7	0.405	0.863	0.523
0.905	0.310	0.720	0.620
1.1	0.208	0.554	0.658
1.3	0.078	0.326	0.497
DESIGN LOADS			
0.905	0.306	0.689	0.606

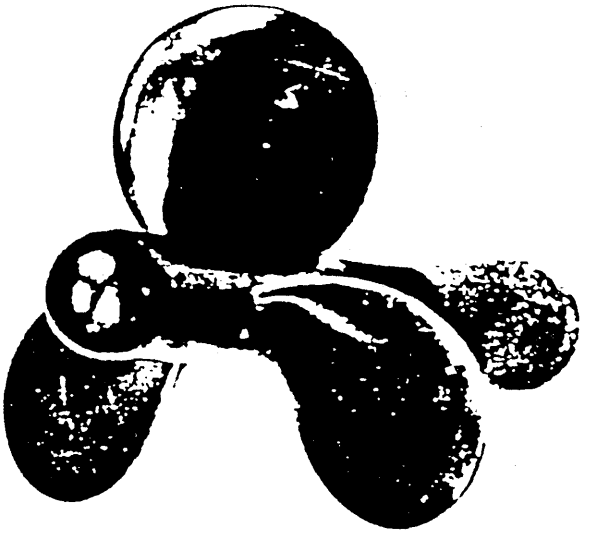

PROPELLER 4119

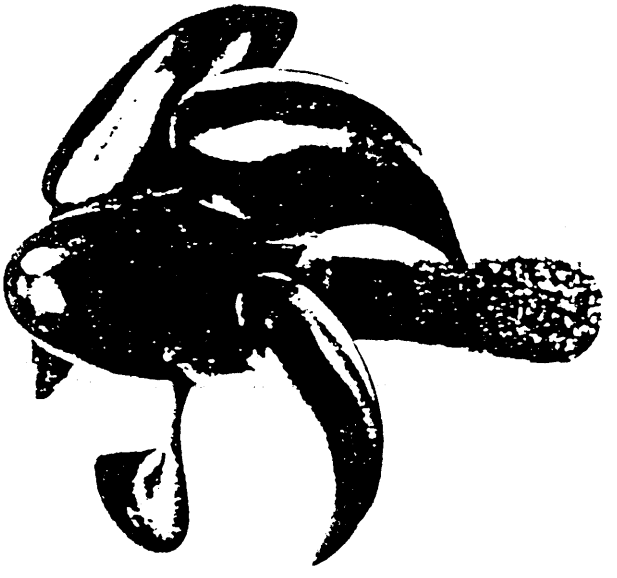

PROPELLER 4842

Fig. 1. 1. 1 Photograph of Proppellers DTRC4119 and DTRC4842

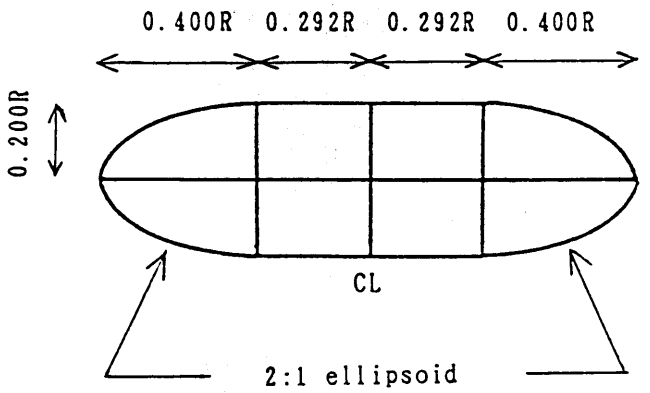

R = propeller radius

DTRC4119

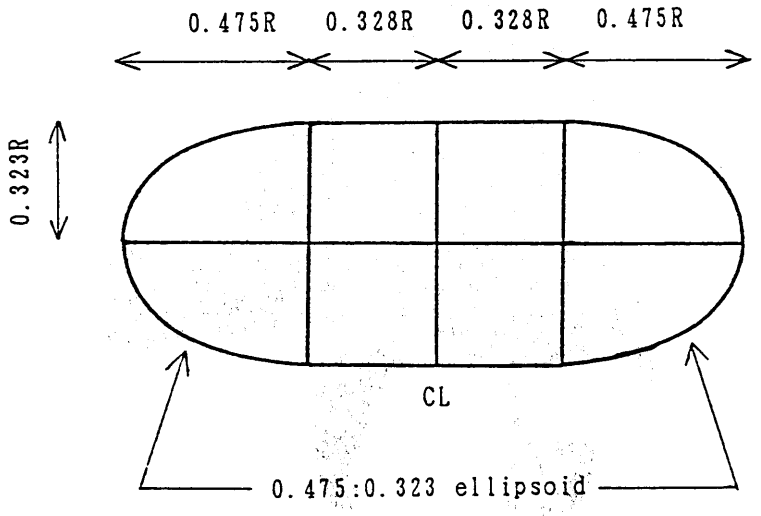

R = propeller radius

DTRC4842

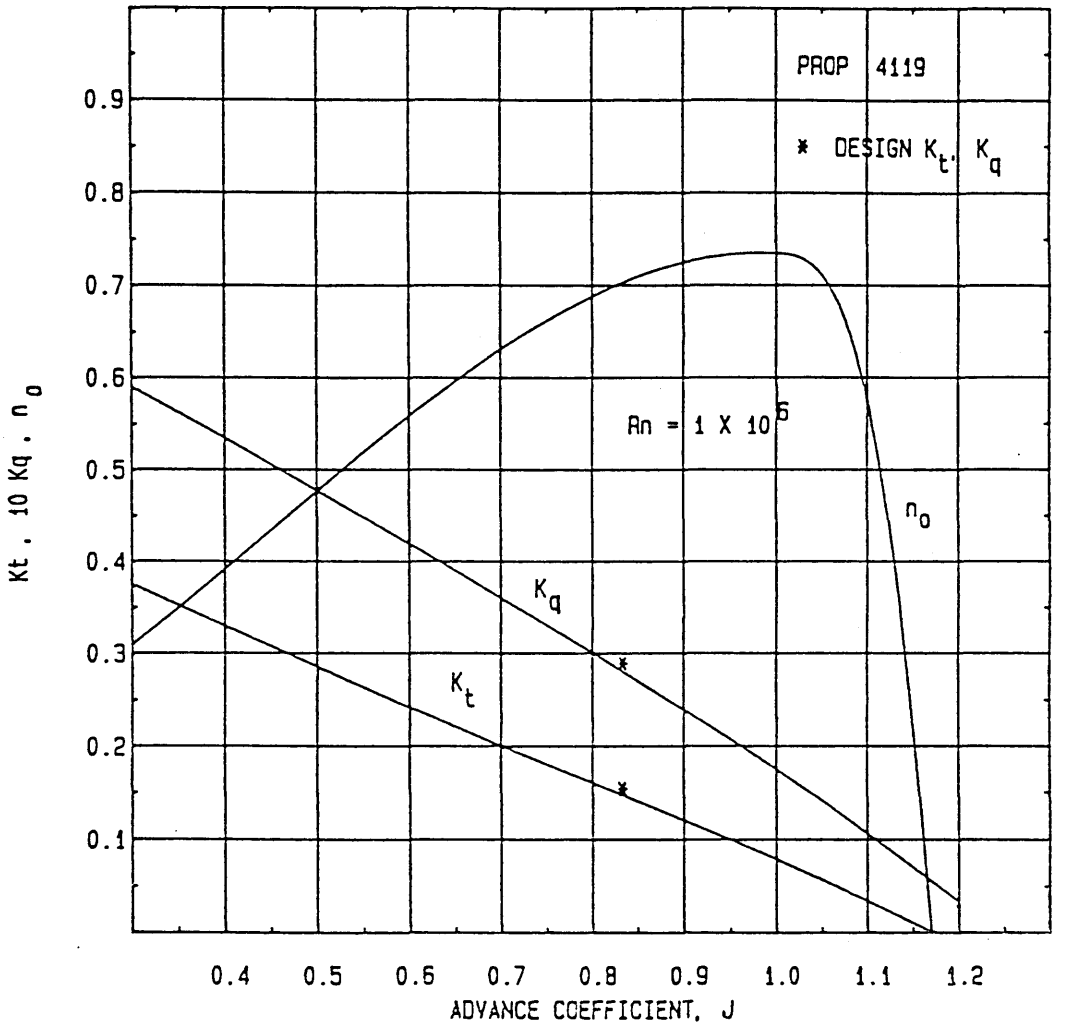

Fig. 1. 3. 1 Open water test results for DTRC4119

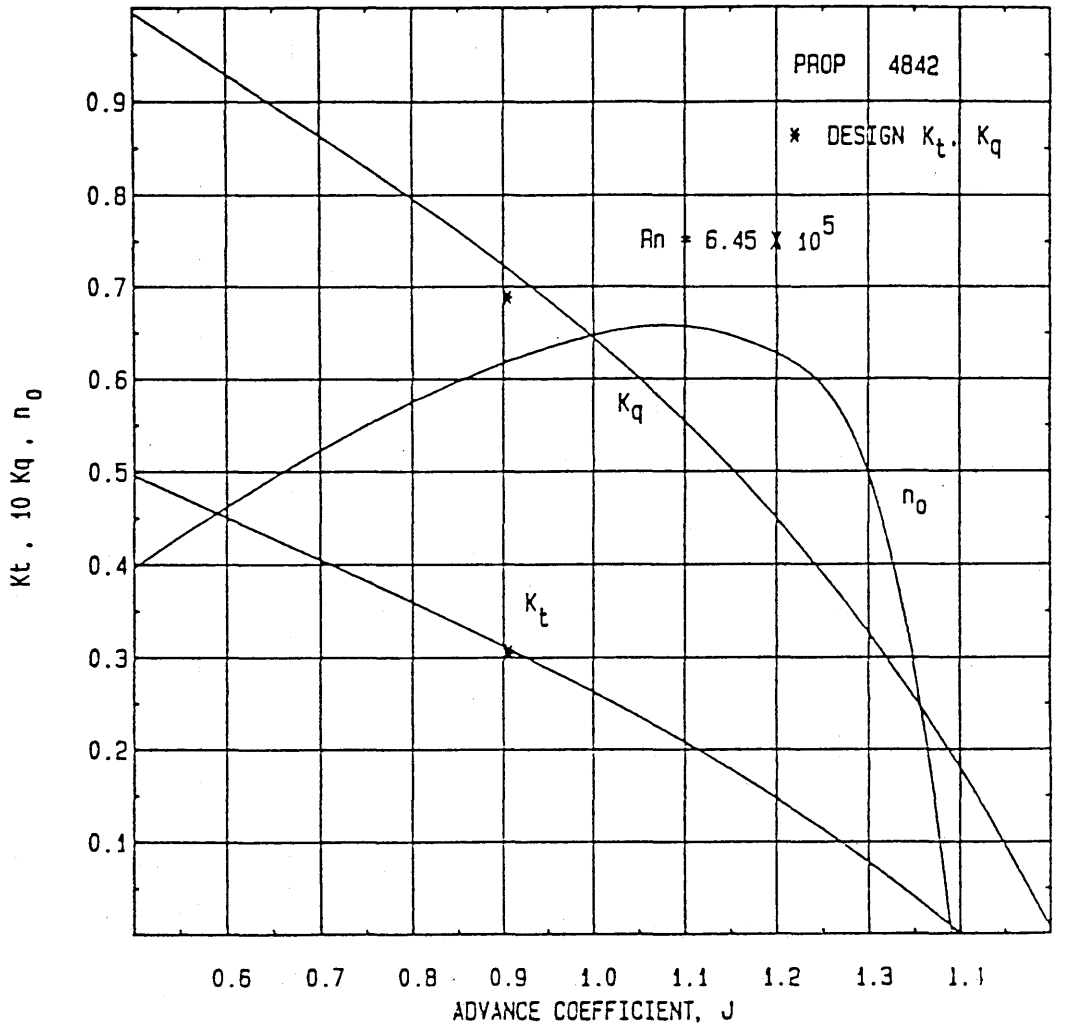

Fig. 1. 3. 2 Open water test results for DTRC4842

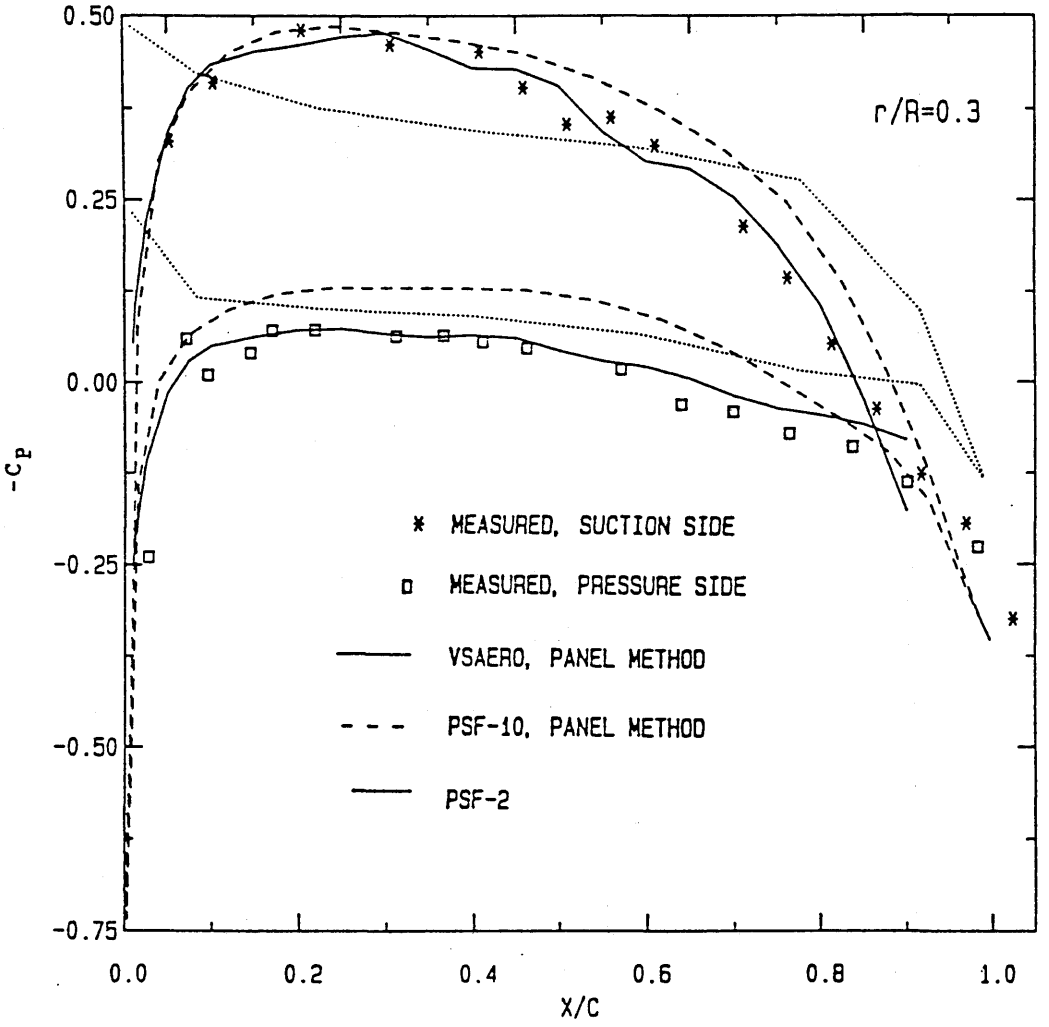

Fig. 1.3.3 (a) Pressure distribution on DTRC4119 (CP at 0.3 radius)

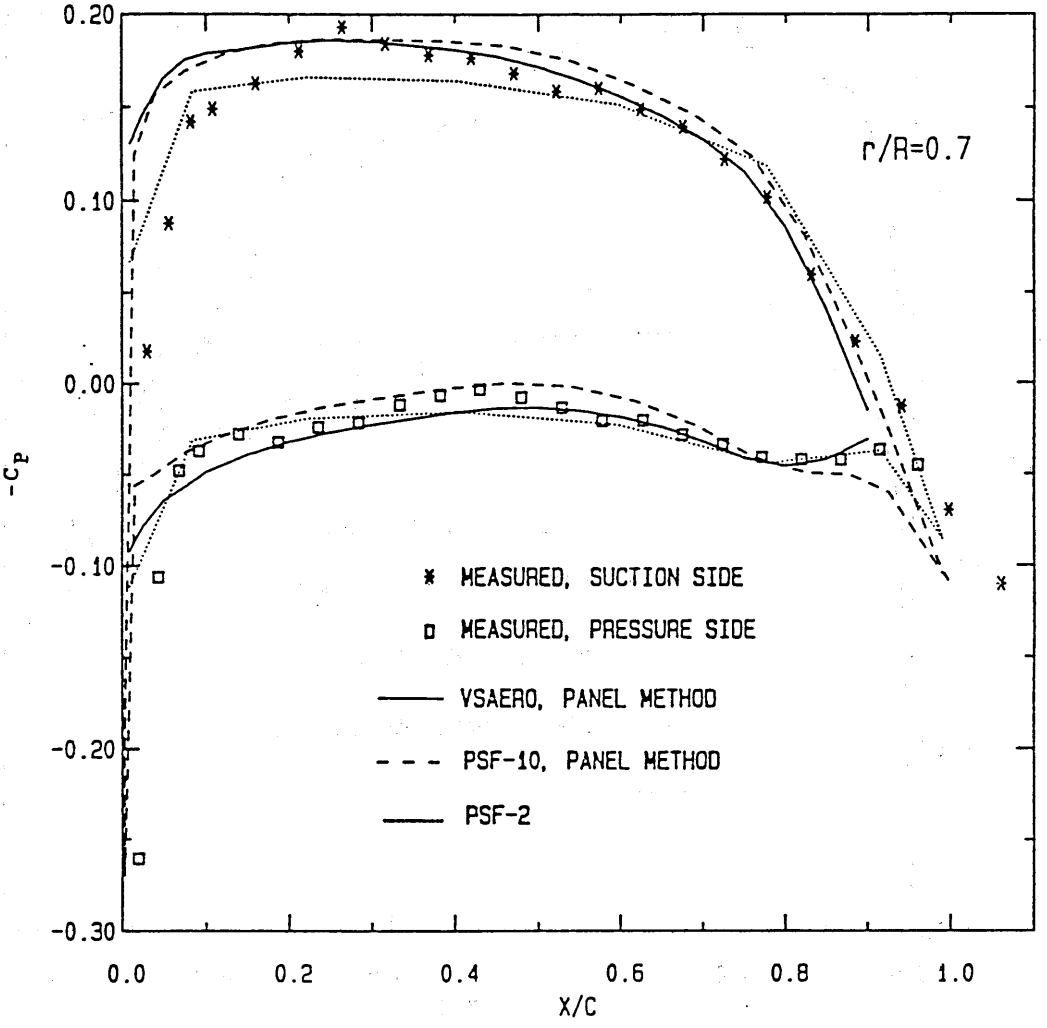

Fig. 1.3.3 (b) Pressure distribution on DTRC4119 (CP at 0.7 radius)

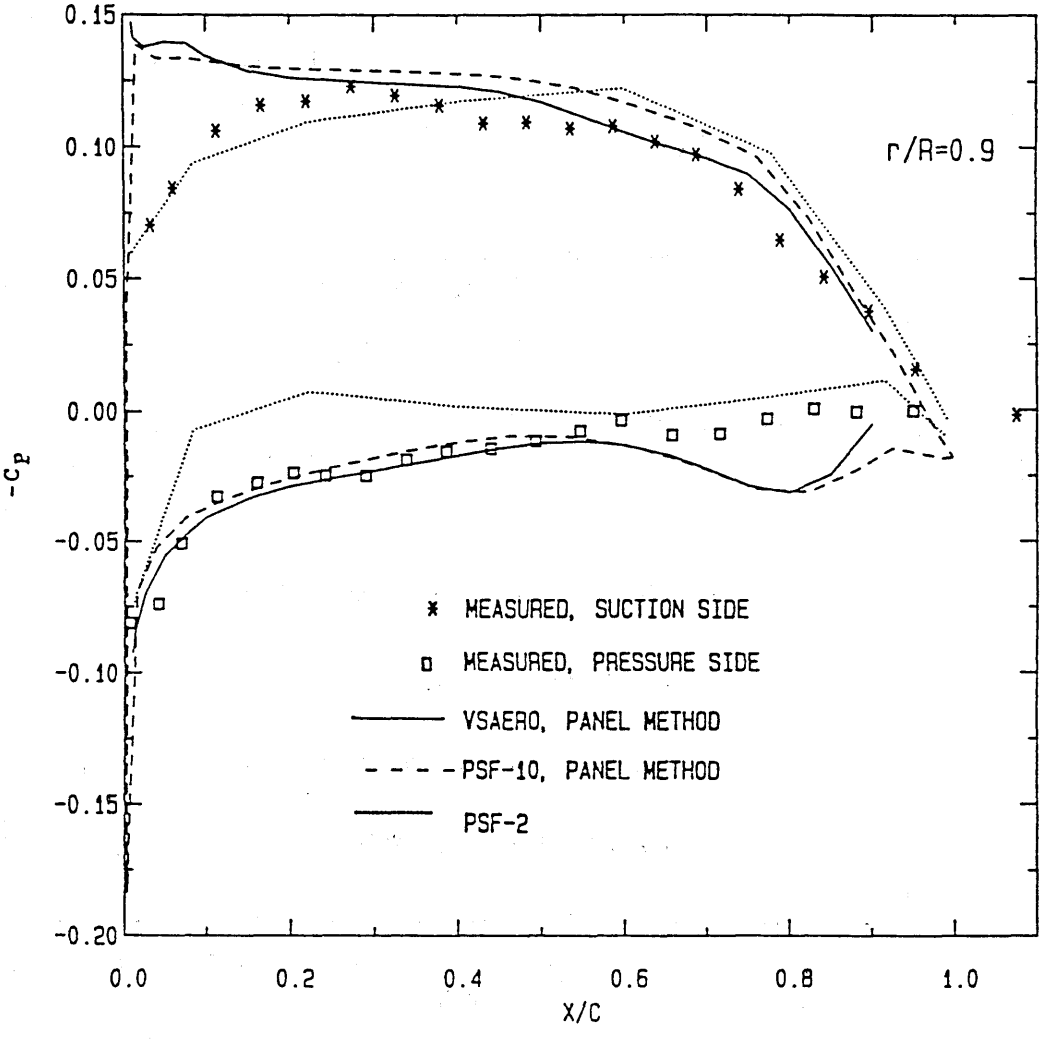

Fig. 1. 3. 3 (c) Pressure distribution on DTRC4119 (CP at 0.9 radius)

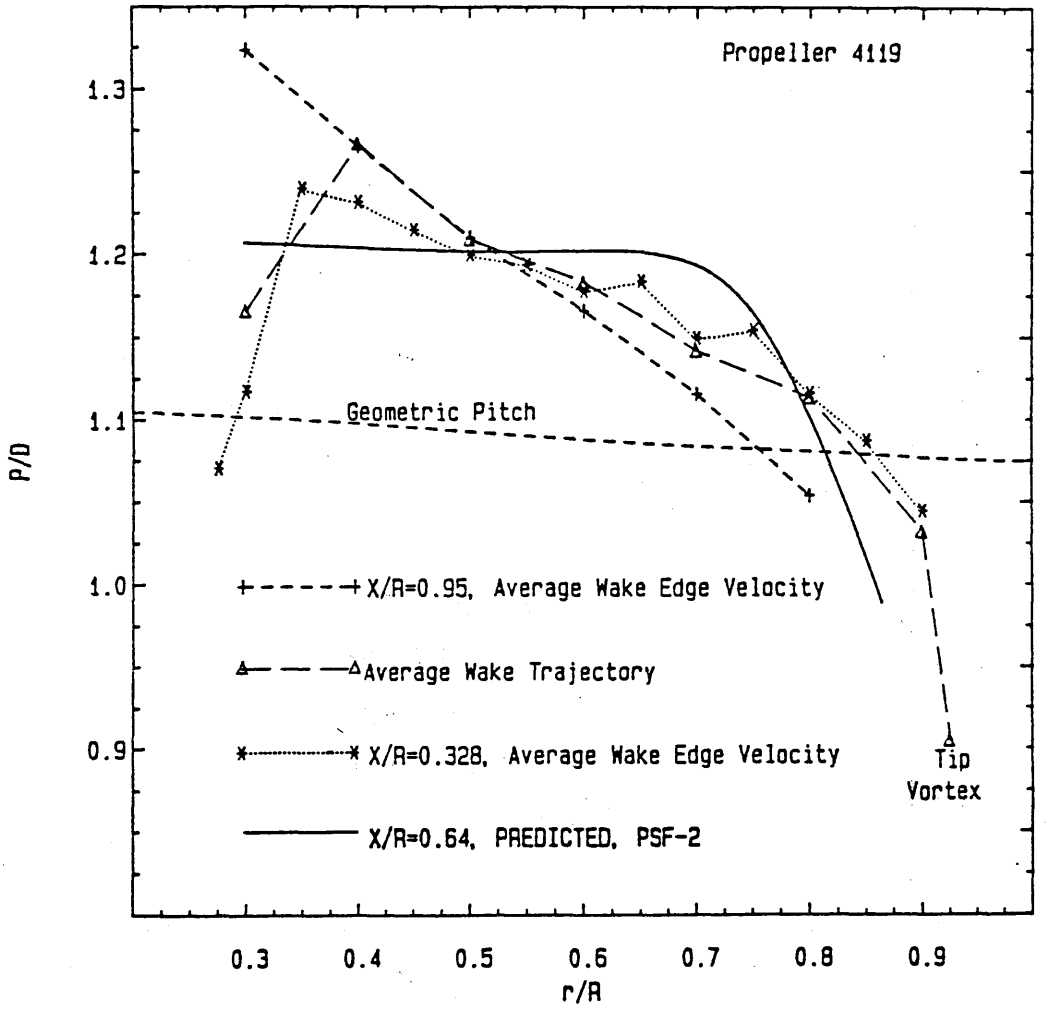

Fig. 1. 3. 4 Distribution of blade wake pitch

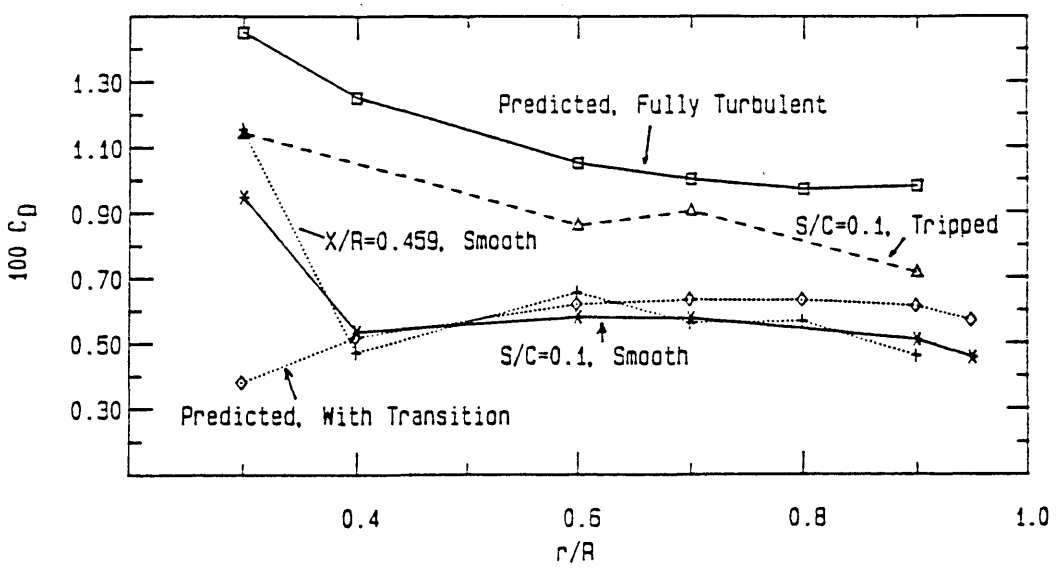

Fig. 1.3.5 Distribution of blade section drag coefficients

The following papers were submitted to the Workshop of ITTC Propulsor Committee. Although these papers contain a lot of valuable and useful information on the panel methods for marine propellers, they are only submitted to the Workshop and they have not been open by any publication. The author believes that it should be very benefitial to researchers of propeller panel methods to publish these papers, and he opens these papers as Appendices of this report with the contributors' permissions. The author would like to thank contributors for permissions.

APPENDIX B

Calculations by DTMB

David Taylor Model Basin
Carderock Division
Naval Surface Warfare Center
carderock, Maryland 20084-5000

Prediction of Hydrodynamic Performance of DTMB Propellers 4119 and 4842 with a Panel Method

Cheng-I Yang

ABSTRACT

This report presents the results of a numerical simulation of the hydrodynamic performance of DTMB Propellers 4119 and 4842. A panel method of analysis is used and the computation code adopted is the DTMB version of the VSAERO code. Numerical prediction includes open water characteristics, pressure distribution on blade surface and velocity at a given plane behind the blade row. Effect of viscous drag correction is also examined. The prediction obtained by panel method agrees reasonably well with the experimental data reported previously by DTMB.

INTRODUCTION

Two open propellers were designed, built and tested extensively in towing basin and water tunnel at DTMB[1]. The physical characteristics of those two propellers are distinctively different. Propeller 4119 is a three bladed propeller with neither rake nor skew. The pitch to diameter ratio of the blade sections remains almost constant from the root to the tip. It has a relatively small hub to diameter ratio (0.2). The design condition of the propeller occurs at advance coefficient , J = 0.833 with a thrust coefficient K_T of 0.154. Propeller 4842 is a five bladed propeller with a moderate degree of rake and skew. The pitch to diameter ratio of blade sections varies significantly from the root to the tip. Its hub to diameter ratio is 0.323. The design advance coefficient is J = 0.905 with a relative high thrust coefficient K_Q of 0.0305. Because of the outlined distinguishing characteristics, the experimental data of these two propellers provide an excellent benchmark for a numerical simulation scheme. The experimental data include; the open water characteristics, surface pressure distribution and the velocity survey behind the propeller. However, because of the obstruction of the optical path by the twisted blade shape of Propeller 4842, information about surface pressure distribution is not available. Comparison of experiment data and computational results obtained by a panel method are presented in following sections.

METHOD OF ANALYSIS

A fluid is incompressible if its particles maintain their density along their paths, i.e., the substantial derivative of mass density ρ is zero:

$$\frac{D\rho}{Dt} = 0 \qquad (1)$$

The principle of mass conservation requires that the net amount of mass flow into a control volume per unit time equal to the rate at which the mass in the control volume is increasing. Thus

$$\frac{\partial \rho}{\partial t} + \nabla \cdot \rho \mathbf{u} = 0. \tag{2}$$

Equation 2 is the differential equation of continuity (the **bold** type denotes a vector quantity). From Eqs. 1 and 2 it follows that for incompressible fluids the equation of continuity is simply

$$\nabla \cdot \mathbf{u} = 0, \tag{3}$$

whether or not the flow is steady and whether or not the fluid is homogeneous. Furthermore, if the density of the fluid is constant and the flow is irrotational, the circulation around a closed circuit is zero,

$$\int \mathbf{u} \cdot d\mathbf{x} = 0. \tag{4}$$

Therefore $\mathbf{u} \cdot d\mathbf{x}$ is an exact differential, which can be denoted by $d\phi$. Thus

$$\mathbf{u} = \nabla \phi. \tag{5}$$

Equations 3 and 5 imply that the function ϕ satisfies the Laplace equation,

$$\nabla^2 \phi = 0 \tag{6}$$

Equation 6 is a kinematics condition; velocity components can be obtained from its solution. The associated pressure, however, can be obtained only from a dynamic condition, that is, the equation of motion. For propeller application, it is more convenient to express the equation of motion with respect to a rotating frame that is fixed to the propeller axis. If the fluid is inviscid and the reference frame is rotating with a constant angular velocity ω about the x axis, Newton's second law governing the flow becomes

$$\frac{D\mathbf{u}}{Dt} + \mathbf{F}_c = -\frac{1}{\rho}\nabla P - \nabla\left(\Omega - \frac{\omega^2 r^2}{2}\right) \tag{7}$$

where $\mathbf{F}_c$ is the Coriolis acceleration vector, Ω is the body force potential, and $r^2 = y^2 + z^2$.

The Coriolis acceleration vector $\mathbf{F}_c$ $(0, -2\omega w, 2\omega v)$ is perpendicular to the velocity vector (u, v, w). Hence its projection onto a streamline is zero. For steady flow of incompressible fluid the density is constant along a streamline S, the equation of motion becomes

$$u_s \frac{\partial u_s}{\partial S} = -\frac{\partial}{\partial S}\left(\frac{P}{\rho} + \Omega - \frac{\omega^2 r^2}{2}\right) \tag{8}$$

Integration of Eq. 8 yields

$$\frac{P}{\rho}+\frac{u_s^2}{2}+\Omega-\frac{\omega^2 r^2}{2}=\text{Constant along a streamline.} \qquad (9)$$

The constant on the right -hand side of Eq.9 can be determined by the upstream condition. It will be invariant throughout the fluid for irrotational flow.

In summary, in deriving Eqs. 6 and 9, it was assumed that (1) the fluid is incompressible and inviscid, the density is constant, and (2) the flow is irrotational and steady. As a consequence, the flow solutions can be obtained from Eqs. 6 and 9, instead of from Eqs. 2 and 7. (Equations 6 and 9 are simplified forms of Eqs.2 and 7.) Equation 6 is linear, with linear boundary condition (without free surface); it can be solved very easily. the velocity components can be determined from Eq. 5 and the associated pressured calculated from Eq. 9. The non linearity of Eq. 7 is reflected only in the non linearity of Eq. 9, and there it presents no difficulty at all because the nonlinear terms are clearly determined and only the pressure is to be evaluated.

Green's theorem is applied to Eq. 6, and then the perturbation velocity potential ϕ_p at a point P on the surface of the propeller can be expressed as follows:

$$2\pi\phi_P=\iint_{S-P}\phi\,\mathbf{n}\cdot\nabla\left(\frac{1}{r}\right)ds+\iint_{W}(\phi_u-\phi_l)\mathbf{n}\cdot\nabla\left(\frac{1}{r}\right)dw$$
$$+\iint_{S}\frac{1}{r}(\mathbf{n}\cdot\mathbf{v}_\infty+\mathbf{n}\cdot\varpi\times\mathbf{R})ds \qquad (10)$$

where
- r =is the length of the vector extended from any other point to the point P and
- S-P =signifies that the point p is excluded from the surface integration;
- **n** =is the normal vector on the surface;
- W =signifies that the surface integration is extended over the wake sheet; and
- ϕ_u, ϕ_l =are the perturbation potentials on the upper and lower sides of the trailing edge, respectively.

The angular velocity of the propeller is ϖ, and **R** is the position vector of point P. The detailed derivation of Eq. 10 is given by Greely and Kerwin[1].

The first term on the right-hand side of Eq. 10 can be interpreted as the potential induced at point P by the distribution of doublets on S-P. their axes lie along the unit normal surface vector **n** and their strength is ϕ on the boundary surface. the same interpretation can be applied to the second term except that the doublet strength is set to $\phi_u - \phi_l$. The third term can be interpreted as the potential induced at point P by the distribution of sources on surface S-P whose strength is determined by the flow condition on the boundary surface. Equation 10 suggests that the strength of the perturbation potential at any given point P on the boundary surface can be considered as a sum of contributions from singularities such as the source and doublet of specified strength placed over the boundary surface of a flow field. Equation 10 can be solved numerically, once the boundary surface is discretized as panels. Therefore, the technique is referred to as a panel method or a singularity method.

The VSAERO code is formulated to solve Eq. 10 numerically to first-order accuracy. It replaces the smooth continuous shape of the body surface with a collection of plane quadrilateral panels and places singularities with constant strengths on the surface

of the plane panels. Some origins of the error associated with the first -order approximation will be outline here.

In general, any four vertices on a curved surface do not determine a plane, that is, the four sides do not rest on a common plane. However, a parallelogram can be formed by joining the four midpoints of the four sides. As a simple approximation, a curved area enclosed by the four vertices can be represented by a plane quadrilateral whose corners are the projections of the vertices onto the plane containing the parallelogram. In order to approximate the continuous physical surface meaningfully with a collection of flat panels, the deviation of the surface points and their projections on the panel plane should be kept as small as possible. The control point of a panel is obtained by taking the algebraic mean of its four corners, but the control point so defined may not lie on the physical surface. the boundary conditions are satisfied only at control points of the panels. Consequently, the velocity components and the potential at the physical surface between the control points are not likely to satisfy the imposed conditions. The difference can be reduced, although it may not be eliminated completely, by a more adaptive panel distribution in which more panels are placed at the region in which the surface normal vector varies rapidly.

The singularities described previously are distributed on the panel surface rather than on the physical surface. For a simple distribution such as the first-order approximation, the influence at a given field point of the singularities of unit strength distributed over a single panel of arbitrary shape can be computed entirely analytically. Such quantities are referred to as influence coefficients. The formation of VSAERO's influence coefficients is described by Newman [2].

When the physical surfaces of the propeller blade are replaced with N flat panels and the wake surface is replaced with M panels, Eq. 10 can be written in a discretized form:

$$2\pi\phi_j = \sum_{\substack{k=1 \\ k\neq j}}^{N}\{C_{jk}\mu_k\} + \sum_{k=1}^{M}\{C_{jk}\mu_k\} + \sum_{k=1}^{N}\{\beta_{jk}\sigma_k\} \qquad (11)$$

where C_{jk} and B_{jk} are the influence coefficients for the constant doublet and source distribution, respectively, on panel k acting on the control point of panel j, and μ_k and σ_k are the strengths of doublet and source on panel k, respective. with σ_k predetermined, Eq. 11 can be written in a matrix form as follow:

$$[\mathbf{A}][\bar{\mu}] = [\mathbf{D}] \qquad (12)$$

where [A] = the influence coefficients matrix,
$[\bar{\mu}]$ = the doublet strength vector, and
[D] = the boundary condition vector.

In actual numerical computation, the assembly of the matrix [A] involves the evaluation of C_{jk} , and the assembly of vector [D] involves the evaluation of B_{jk} . This process is very time consuming. [A] is a full matrix, and the solution of Eq.12 requires a large portion of the total computing effort, especially when the panel number is large.

In VSAERO code, the block Gauss- Seidel method is used for solving the system of equation in Eq.12. Once the potential field is obtained, the velocity components at each control point can be obtained by a finite-differencing scheme. In VSAERO code, the values of the potential at four surrounding control points are used as a base for finite-

differencing, and the method is of first-order accuracy. The pressure distribution on the surface is obtained by applying the steady-state Bernoulli equation.

PROPELLER 4119

The geometrical definition of the blade and the hub is given in reference 3. For numerical modelling, the blade surface is divided into 10 spanwise sections; each section contains 58 panels. The distribution of the panels is nonuniform in order to accommodate the surface curvature variation and to reduce the numerical error. The hub surface between two adjacent blades is modelled by 152 panels, there are 19 panels in axial direction and 8 panels in circumferencial direction. In present model, the corner points of the bounding panels from the blade and the hub match at the intersection. The hub surface in front of the blade row is modelled with 240 panels; there are 10 panels in axial direction and 24 panels in circumferencial direction. The surface behind the blade row is modelled by 240 panels. Over all a total of 2,556 panels are used to model this three bladed propeller. The perspective views of the discretized propeller is shown in Figure 1.

Two wake models are used for computations. The linear wake has no contraction. For a given wake line, its pitch angle is set to equal to the geometrical pitch angle of the blade section from where the wake line emanates. The deformed wake has contraction. The contraction model follows the suggestion by Hoshino [4]. For a given wake line, its pitch angle is aligned with the velocity at the trailing edge of the blade section from where the wake line emanates. To derive the deformed wake , an iteration process is required.

The viscous effect is accounted for through the specified sectional drag coefficient. The frictional coefficient is calculated using the 1957 International Towing Tank Conference Correlation Line. The total drag coefficient is calculated using empirical corrections given by Abbot and Von Doenhoff [5].

OPEN WATER CHARACTERISTICS

The comparison of the computed and the experimental open water characteristics is shown in Figure 2. Two sets of computational results are presented. In both cases, the deformed wake model are used. In one case the viscous correction is applied while in the other it is not. The purpose of this computation is twofold; the first is to examine the ability to predict the thrust and torque over a range of advance coefficient and the second is to examine the effect of the viscous correction. In view of the results presented in Figure 2, it appears that with the viscous drag correction, the thrust and torque can be predicted reasonably well over a wide range of advance coefficient. It also shows that in the absence of the viscous correction, the torque is considerably under predicted.

In order to examine the effect of the hub on the performance prediction, the hub panels are removed and the blade root is patched up with flat panels. The results are shown in Figure 3. Compared with the case with the hub, the differences in predicted thrust and torque are very slight over the range of advance coefficient studied.

The linear wake model has also been used to repeat the computations and it yields practically identical results.

SURFACE PRESSURE DISTRIBUTION

In reference 3, the surface pressure distribution at a given radial position was derived from the velocity components measured near the blade surface with a LDV technique. The derivation followed the inviscid steady-state Bernoulli's equation. In present analysis, the pressure distribution was derived in the similar manner. First, the velocity components were obtained by finite differencing the values of the potential on

blade surface, and then the pressure was obtained by applying the Bernoulli's equation. These approaches adopted in the experiment and in the analysis are compatible and valid under the condition that the blade boundary layer is thin and remains attached. The comparison between the experimental data and the computational results is meaningful only if such condition is fulfilled. Therefore, it is expected that the agreement will be better at the mid-span than at the root or the tip regions.

Surface pressure distributions at several radii are presented in Figure 4. The agreement between the computational results and the experimental data are good The hub effect is significant only at the inner most radius. Both the linear and the deformed wake model were used to perform the computations, the differences in surface pressure distributions are negligible.

VELOCITY COMPONENT BEHIND THE PROPELLER

In order to study the effect of the wake models on the flow field prediction, results from two computations at design advance coefficient are presented. One is obtained with linear wake model and the other is obtained with deformed wake model. Figures 5-6 display the results. The plane on which the velocity components are computed is located at 1.77 inches behind the propeller centerline (x/R = 0.295). Figure 1 shows the relative location of this plane with respective to the blades. The view is from downstream toward upstream and the propeller rotates in clockwise direction. The vortices shed from the blade tips can clearly be identified from the cross flow vector plot. However, different wake models predict different locations for the tip vortices. The deformed wake model predicts tip vortices slightly inboard in the radial direction and further downstream in the circumferencial direction. This is caused by the contraction of the wake lines.

The comparison of the computed and the measured velocity components at axial location x/R = 0.295 and radial location r/R = 0.7 is shown in Figure 7. In present case , the linear wake is used. The advance coefficient is J = 0.806. The agreement between the computed and the measured values is very good except at the regions where the viscous boundary layer is dominating.

PROPELLER 4842

The surface of Propeller 4842 is replaced with panels in the same manner as is described for propeller 4119. A total of 4,260 panels are used to model this five bladed propeller. The perspective views of the discretized propeller are shown in Figure 8 .The after portion of the hub of the test model was truncated and attached to a shaft with a smaller diameter. The panel model reflects this adjustment.

OPEN WATER CHARACTERISTICS

The prediction of open water performance is shown in Figures 9-10. Figure 9 indicates the degree of the viscous effect while Figure 10 shows the degree of the hub effect upon the performance prediction. The hub effect is insignificant at a lower but important at a higher advance coefficient. In all computations the deformed wake model and the viscous correction are implemented.

SURFACE PRESSURE DISTRIBUTION

Figure 11 show the prediction of the surface pressure distribution at various radius positions at the design advance coefficient. It is indicated in the figures that the effect of hub fades rapidly as the radius increases.

VELOCITY COMPONENTS BEHIND THE PROPELLER

Velocity components at a plane behind the propeller were measured [1]. The plane is located at 2.44 inches (x/R = 0.344) from the centerline of the blades. It is about the same axial location where the truncated hub joints the driving shaft. A backward facing step is formed and flow separation is expected. The impact on flow field prediction with a panel method is unclear. The relative location of the velocity measuring plane and the propeller blades is shown in Figure 12. Comparison of computed and measured values at radial position r/R = 0.822 is shown in Figure 13. The agreement is only fair. Cross flow velocity vector and axial velocity contour on that plane are shown in Figure 14-15 respectively. Tip vortices are not as well defined as that of Propeller 4119.

ACCURACY OF THE SIMULATIONS AND THE EXPERIMENT

Numerical simulation is an attempt, with the assistance of mathematics and physics and the resource of modern computers, to predict a physical phenomenon in a discretized manner. At present, one of the most popular approaches involves describing the phenomenon with an equivalent mathematical model and obtaining the solution with a discretization technique. The simulation technique of the panel method presented in this report is an example of this approach. The phenomenon involving fluid dynamics can best be described by the Navier-Stokes equation with an appropriate turbulence model. In formulating the equations various assumptions have been made and the final form is nonlinear. By imposing certain conditions on the flow field, such as those of Eq. 6 and Eq. 9, the non linearity can be removed from the mathematical model. However, the application of the model becomes further restricted and perhaps one more step away from the physical reality. The formulation outlined in the previous sections lead us to expect only first-order accuracy from the results of the panel method code VSAERO. Discretization techniques create yet another source of error. Detailed accounts of the effect of the mathematical accuracy on the physical prediction are discussed in references 6 and 7.

At present simulations, about 852 panels are used to model each blade sector of a propeller. Two sets of paneling with their control points positioned at different locations were modeled. For both sets of paneling, the total number of panels was the same and the panel distributions were nonuniform and curvature-adapted. the difference in computed thrust is approximately 2%.

In experiment, the propeller rotation speed was maintained to within 0.5% while the tunnel speed was maintained to within 1%. The accuracy in which the LDV measuring point was positioned produced errors in the measured results. Overall positioning accuracy was influenced by errors in referencing position, accumulated errors after referencing, and errors occurring when the transmitting beam axis was not perpendicular to the tunnel window. The axial and vertical reference was accurate to within approximately 0.003 inch (0.075 mm)and the y axis reference was accurate to within 0.030 inch (0.75mm). The accumulation of the traverse error was within 0.01 inch (0.25 mm). The calibration of the fiber optic probe was checked by measuring free stream velocity with both optical systems with agreement to within 0.2%.

CONCLUSION

Numerical simulations of the hydrodynamics performance of Propellers 4119 and 4842 with a panel method were performed and the results are presented. It is observed that :

(1) The linear wake model and the deformed wake model predict different locations for the tip vortices.
(2) Wake models have insignificant effect on the thrust and torque prediction.
(3) Viscous drag correction is essential to the correct prediction of the torque. Its effect on the prediction of the thrust is marginal.
(4) The effect of the hub on performance prediction depends not only on its size (hub to diameter ratio) but also the advance coefficient at which the propeller operates.
(5) Panel method predicts the hydrodynamic performance of open propellers well, if the rake and skew are relatively moderate.

REFERENCES

[1] Greely, D.S., Kerwin, J.E."Numerical Method for Propeller Design in Steady Flow," SNAME Transactions, Vol. 90 1982.

[2] Newman, J.N. "distributions of Sources and Normal Dipoles over a Quadrilateral Panel," Journal of Engineering Mathematics Vol 20 1986 pp113-126

[3] Jessup, S.D. "An Experimental Investigation of Viscous Aspects of Propeller Blade Flow," Ph.D. Dissertation. The Catholic University of American. 1989

[4] Hoshino, T. "A Surface Panel Method with a Deformed Wake Model to Analyze Hydrodynamic Characteristics of Propeller in Steady Flow," Mitsubishi Technical Bulletin No.195 April 1991.

[5] Abbot,I.H., von Doenhoff, A.E., "Theory of Wing Sections" Dover Publications Inc., New York (1949)

[6] Maskew, B.," Prediction of Subsonic Aerodynamic Characteristics : a Case of Low-Order Panel Method," J. of aircraft, Vol. 10, No. 2 February 1982

[7] Oskem, B.," Asymptotic convergence of High-Order Accurate Panel Method," NLR MP 85043 U April 1985